RERTR 2008 — 30th INTERNATIONAL MEETING ON REDUCED ENRICHMENT FOR RESEARCH AND TEST REACTORS

October 5-9, 2008
Hamilton Crowne Plaza Hotel
Washington, D.C. USA

PREDICTIVE MODELING OF SOLUTION CHEMISTRY IN AN AQUEOUS HOMOGENEOUS REACTOR USED FOR MO-99 PRODUCTION

James L. Jerden Jr. and George F. Vandegrift
Argonne National Laboratory
9700 South Cass Avenue
Argonne, Illinois 60439-4837 U.S.A.

ABSTRACT

Thermodynamic models of the solution chemistry in a homogeneous reactor used for molybdenum-99 production are being developed at Argonne to aid in the optimization of molybdenum generation and recovery processes. The models calculate concentrations of aqueous species and saturation states of possible uranium and fission product precipitates (e.g., uranyl oxide hydrates, peroxides, molybdates) over a relevant range of pH, oxidization/reduction potential and component concentrations. Predicting conditions under which precipitation may occur is particularly important because solids formed in the reactor solution could complicate molybdenum-99 recovery and have deleterious effects on reactor operation. Results presented in this paper indicate that, for uranyl nitrate based reactors, the radiolytic decomposition of nitrate (loss of nitrogen to off-gas) could cause the precipitation of uranyl and/or fission products due to an increase in pH. This precipitation process is readily counteracted by the addition of nitric acid. The modeling results presented help quantify the optimal pH envelope for a uranyl nitrate solution reactor used for molybdenum-99 production and highlight the need for future experimental studies to address uncertainties in the thermodynamic models.

1. Introduction

Thermodynamic speciation and reaction path modeling can be used to optimize the production of molybdenum using a homogeneous aqueous reactor. Such models can be used to determine optimal conditions (e.g., pH, composition, reduction/oxidation potential) for both reactor operation and subsequent molybdenum separation steps (e.g., anion exchange). For reactor operation, one of the key questions that can be addressed by modeling is, what is the saturation state of the reactor solution with respect to uranium and molybdenum solids? It is important to be able to predict the conditions at which uranium and molybdenum solids will precipitate as such solids may affect reactor neutronics and lower molybdenum recovery efficiency. For the

downstream molybdenum separation processes a key question that can be addressed by modeling is, what is the speciation of molybdenum and fission products and how will their speciation influence separation efficiency? Speciation is important because it determines the uptake efficiency of molybdenum on anion exchange columns. For example, $HMoO_4^-$ or MoO_4^{2-} may be readily adsorbed by the resin, while MoO_2^{+} or $ZrMoO_2^{2+}$ may not. Furthermore, the presence of fission product anions such as TcO_4^-, IO_3^-, I^-, Br^-, $HSeO_4^-$ and SeO_4^{2-} may compete with $HMoO_4^-$ or MoO_4^{2-} on anion exchange resins and thus lower the molybdenum separation efficiency and influence product purity.

This paper presents results from thermodynamic modeling that address these precipitation and speciation issues for a hypothetical solution reactor with fuel consisting of 1 molar uranyl nitrate and 0.1 molar nitric acid (operating at 1 bar pressure). Although such a reactor would likely be operating at a temperature near 80°C, the results presented are from models run at 25°C. The 25°C models are deemed more accurate due to a scarcity of thermodynamic data for key species at higher temperatures and evidence that a temperature difference of 55°C would not dramatically affect speciation. The concentrations of the actinides and fission products in the model system are shown in Table 1. Theses concentrations were calculated using the ORIGEN code for a reactor that is run for 365 days at 200 kW in 7 day cycles [1]. Each cycle consisted of 5 days of 200 kW operation followed by a 2 day cooling period [1]. The total molybdenum concentration was fixed at $1x10^{-5}$ molar, which approximates the concentration that would result from regular separation from the solution.

Table 1. Molar (moles/L) concentrations of elements in the model reactor solution immediately after being discharged from the reactor and after a 48 hour cooling period. The molybdenum concentration was fixed to reflect its being removed from the system regularly.

Element	After Discharge	After 48 hours cooling	Element	After Discharge	After 48 hours cooling
Uranium	1.0	1.0	Rhodium	$4.7x10^{-5}$	$4.8x10^{-5}$
Zirconium	$5.4x10^{-4}$	$5.4x10^{-4}$	Tellurium	$4.1x10^{-5}$	$4.0x10^{-5}$
Molybdenum	$1.0x10^{-5}$	$1.0x10^{-5}$	Samarium	$3.9x10^{-5}$	$3.9x10^{-5}$
Cesium	$3.5 x10^{-4}$	$3.5 x10^{-4}$	Promethium	$3.5x10^{-5}$	$3.5x10^{-5}$
Neodymium	$3.1 x10^{-4}$	$3.1 x10^{-4}$	Palladium	$2.6x10^{-5}$	$2.6x10^{-5}$
Cerium	$3.0 x10^{-4}$	$3.0 x10^{-4}$	Iodine	$1.8x10^{-5}$	$1.7x10^{-5}$
Ruthenium	$2.2 x10^{-4}$	$2.2 x10^{-4}$	Niobium	$1.6x10^{-5}$	$1.6x10^{-5}$
Strontium	$1.9 x10^{-4}$	$1.9 x10^{-4}$	Selenium	$9.8x10^{-6}$	$9.8x10^{-6}$
Plutonium	$1.7x10^{-4}$	$1.7x10^{-4}$	Boron	$8.8x10^{-6}$	$8.8x10^{-6}$
Barium	$1.3x10^{-4}$	$1.3x10^{-4}$	Europium	$3.6x10^{-6}$	$3.6x10^{-6}$
Lanthanum	$1.2x10^{-4}$	$1.2x10^{-4}$	Bromine	$3.6x10^{-6}$	$3.6x10^{-6}$
Technetium	$1.2x10^{-4}$	$1.2x10^{-4}$	Neptunium	$3.1x10^{-6}$	$2.2x10^{-6}$
Praseodymium	$9.9x10^{-5}$	$9.9x10^{-5}$	Tin	$2.5x10^{-6}$	$2.5x10^{-6}$
Yttrium	$9.7x10^{-5}$	$9.7x10^{-5}$	Cadmium	$1.6x10^{-6}$	$1.6x10^{-6}$
Rubidium	$6.5x10^{-5}$	$6.5x10^{-5}$	Antimony	$1.1x10^{-6}$	$1.0x10^{-6}$

***Only elements with concentrations ≥ $1x10^{-6}$ molar were modeled.**

2. Methods

Thermodynamic models were implemented using the codes OLI ESP Stream Analyzer (OLI-SA) and "The Geochemist's Workbench®" Release 3.0 (GWB). The thermodynamic databases used for the OLI-SA modeling were the "Geochemical", "Corrosion" and "Public". The thermodynamic database used for modeling with GWB was an adapted version of the database "thermo.com.V8.R6.full" [2] to which relevant thermodynamic data for molybdenum species [3] were added by the authors. In general, both modeling codes use a Gibb's free energy minimization technique to determine the equilibrium state of the system of interest. More specifically, the codes use equilibrium constants for a set of basis reactions to solve a matrix of mass and charge balance equations. Results from these calculations feed into an iterative algorithm that converges on a unique equilibrium state for the multicomponent, multiphase system of interest.

The saturation state of the solution was calculated using the saturation index (SI), which is defined as: $SI = \log_{10}(Q/K_{eq})$, where Q is the reaction quotient ($Q = [C]^c[D]^d/[A]^a[B]^b$ for the reaction $aA + bB \leftrightarrow cC + dD$, where brackets indicate concentration in moles per liter). The reaction quotient, which changes continuously during the reaction until equilibrium is achieved is related to the Gibbs free energy of the reaction by: $\Delta G_r = \Delta G_r^o + RT \ln Q$; where ΔG_r is the Gibb's free energy change over the reaction, ΔG_r^o is the Gibbs free energy change for the reaction at standard state (298.15K, 1 bar, activity of solutes equal to 1.0), R is the gas constant, and T is absolute temperature. At equilibrium Q becomes constant and equal to the equilibrium constant (K_{eq}), and ΔG_r goes to zero. The equilibrium constant is defined by: $\Delta G_r^o = -RT \ln K_{eq}$. Therefore, at equilibrium, SI = 0 and, if the reaction is written with the solid phase as a reactant, if SI < 0, the solution is undersaturated with respect to that mineral and if SI > 0 the solution is supersaturated.

The oxidation/reduction potential of the reactor solution was also calculated and is one of the dominant controls on speciation for redox sensitive elements such as uranium and molybdenum (e.g., it determines the ratio $HMoO_4^-/MoO_2^+$). In the models discussed below the redox conditions are quantified as Eh, which is the oxidation/reduction potential of the solution (in volts) relative to the standard hydrogen electrode. For the reaction $aA + bB + ne^- \leftrightarrow cC + dD$ the Eh is defined as: $Eh = E^o + (RT/nF) \ln([A]^a[B]^b/[C]^c[D]^d)$, where E^o is the standard potential of the reaction in volts, R is the gas constant, T is absolute temperature, n is the number of electrons transferred, and F is the Faraday constant.

3. Results and Discussion

The equilibrium speciation of the reactor solution was calculated using OLI-SA at 25°C is shown in Table 2. The equilibrium pH, oxidation/reduction potential (Eh) and density are predicted to be 1.18, 1.1 volts and 1.3 g/mL respectively. This equilibration was also run at 80°C and it was found that there was little change in the aqueous properties or speciation other than the absence of some complexes for which higher temperature data is not yet available. The major differences for the solution at 80°C are that the H^+ activity coefficient decreases to 0.59 and the pH increases to 1.23 (most of the models discussed below were run at 25°C due to a lack of thermodynamic data for relevant species at higher temperatures). At 25°C, the solution is saturated with respect

to tin oxide (SnO_2). Some of the key cationic species include: the uranyl ion, uranyl hydroxide, zirconium hydroxide, lanthanide nitrates, plutonyl(VI) nitrate, plutonyl(VI), neptunyl(V), uranyl iodate and zirconium molybdate. It should be noted that uranyl nitrate (UO_2NO3^+) is not included in the OLI databases; however, the GWB models, discussed below, predict that uranyl nitrate is an important cationic species. The main neutral species include: cesium and strontium nitrates and plutonyl(VI) dinitrate. The dominant anions include: nitrate, pertechnetate, selenate, hydrogen selenate, hydrogen molybdate, bromide and iodate (Table 2).

The relatively high concentration of zirconium molybdate is of specific interest because it implies that, at a pH of 1.18, around half of the molybdenum is present in a cationic state. This could potentially lower molybdenum recovery by anion exchange. However, the stability constant for the zirconium molybdate complex appears to be uncertain as it is not included in many of the standard thermodynamic compilations for molybdenum (e.g., [3], [4]). This uncertainty should be considered a key target for future work.

Table 4: Equilibrium speciation of reactor solution at 25°C (starting concentrations are from Table 1).

Aqueous Properties					
Temperature (°C)	25.0				
pH	1.18				
(H^+) activity coefficient	0.699				
Eh* (volts)	1.1				
Density (g/mL)	1.3				
Phase Amounts	(moles)	(grams)			
Aqueous	58.2	1390.7			
Solids	$2.3E^{-6}$	$3.5E^{-4}$			
Solids	(moles)	(grams)	**Aqueous** (cont.)	(molar)	(mg/kg)
SnO_2	$2.3x10^{-6}$	$3.5x10^{-4}$	Pd^{2+}	$2.1x10^{-5}$	1.64
Aqueous	(molar)	(mg/kg)	$UO_2IO_3^+$	$1.7x10^{-5}$	5.46
NO_3^-	2.1	$9.4x10^{+4}$	$SmNO_3^{2+}$	$8.9x10^{-6}$	1.36
UO_2^{2+}	1.0	$1.9x10^{+5}$	$B(OH)_3$	$8.8x10^{-6}$	0.39
H^+	$9.4x10^{-2}$	68.0	$LaNO_3^{2+}$	$8.6x10^{-6}$	1.25
$ZrOH^{3+}$	$2.7x10^{-4}$	20.8	$ZrMoO_4^{2+}$	$6.8\ x10^{-6}$	1.2
$NdNO_3^{2+}$	$2.3x10^{-4}$	33.7	SeO_4^{2-}	$6.3x10^{-6}$	0.65
$CeNO_3^{2+}$	$2.2x10^{-4}$	32.5	Br^-	$3.5x10^{-6}$	0.20
Ru^{3+}	$2.2x10^{-4}$	16.0	$HSeO_4^-$	$3.5x10^{-6}$	0.36
$CsNO_3$	$2.1x10^{-4}$	29.4	$HMoO_4^-$	$3.2x10^{-6}$	0.36
Cs^+	$1.4x10^{-4}$	13.0	Y^{3+}	$3.2x10^{-6}$	0.21
Ba^{2+}	$1.3x10^{-4}$	12.8	$PdOH^+$	$3.2x10^{-6}$	0.28
TcO_4^-	$1.1x10^{-4}$	12.9	NpO_2^+	$2.9x10^{-6}$	0.57
La^{3+}	$1.1x10^{-4}$	10.9	$EuNO_3^{2+}$	$2.8x10^{-6}$	0.43
$(UO_2)_2(OH)_2^{2+}$	$1.0x10^{-4}$	42.8	HNO_3	$1.7x10^{-6}$	0.08
$Sr(NO_3)_2$	$9.5x10^{-5}$	15.0	$Pd(OH)_2$	$1.4x10^{-6}$	0.14
Nd^{3+}	$8.2x10^{-5}$	8.6	MoO_4^{2-}	$1.2x10^{-6}$	0.14
Ce^{3+}	$7.6x10^{-5}$	7.7	Cd^{2+}	$9.1x10^{-7}$	0.07
$PuO_2(NO_3)_2$	$6.9x10^{-5}$	19.9	Eu^{3+}	$8.5x10^{-7}$	0.09
$PuO_2NO_3^+$	$6.7x10^{-5}$	16.2	$CdNO_3^+$	$6.9x10^{-7}$	0.09
$PrNO_3^{2+}$	$6.6x10^{-5}$	9.6	IO_3^-	$6.5x10^{-7}$	0.08
$Y(NO_3)_2^+$	$6.5x10^{-5}$	9.9	$Sb(OH)_5$	$5.5x10^{-7}$	0.08
Rb^+	$6.5x10^{-5}$	4.0	$RuOH^{2+}$	$4.1x10^{-7}$	0.04
$SrNO_3^+$	$5.9x10^{-5}$	6.4	H_3SbO_4	$4.0x10^{-7}$	0.05
Zr^{4+}	$4.9x10^{-5}$	3.2	HIO_3	$2.9x10^{-7}$	0.04
Rh^{2+}	$4.8x10^{-5}$	3.6	$Pu(NO_3)_4$	$2.7x10^{-7}$	0.09
Sr^{2+}	$4.6x10^{-5}$	2.9	$Pu(NO_3)_3^+$	$1.8x10^{-7}$	0.05
$Te(OH)_3^+$	$4.1x10^{-5}$	5.3	$Zr(OH)_2^{2+}$	$1.6x10^{-7}$	0.01
PuO_2^{2+}	$3.3x10^{-5}$	6.6	$Sn(OH)_4$	$1.0x10^{-7}$	0.01
Pr^{3+}	$3.3x10^{-5}$	3.4			
UO_2OH^+	$3.2x10^{-5}$	6.6			
Sm^{3+}	$3.0x10^{-5}$	3.2			
YNO_3^{2+}	$2.9x10^{-5}$	3.2			

***Eh: the oxidation/reduction potential (in volts) of the solution relative to the standard hydrogen electrode.**

To establish a general context for how changes in redox conditions and hydrogen ion activity could influence the speciation of the reactor solution, Eh vs. pH diagrams were plotted for the system of interest. Examples for some of the key elements (i.e. uranium, molybdenum and iodine) are shown in Figure 1. These diagrams, which show the predicted equilibrium Eh – pH conditions for the reactor solution as yellow circles, indicate that the uranyl ion, uranyl nitrate, hydrogen molybdate, iodate and uranyl iodate are predicted to be dominant species. They also imply that if the Eh of the solution decreases, perhaps due to radiolysis or hydrogen production, the speciation of molybdenum and iodine could be significantly affected. For example, hydrogen molybdate could be reduced to MoO_2^+ and iodate could be reduced to I_2 or iodide.

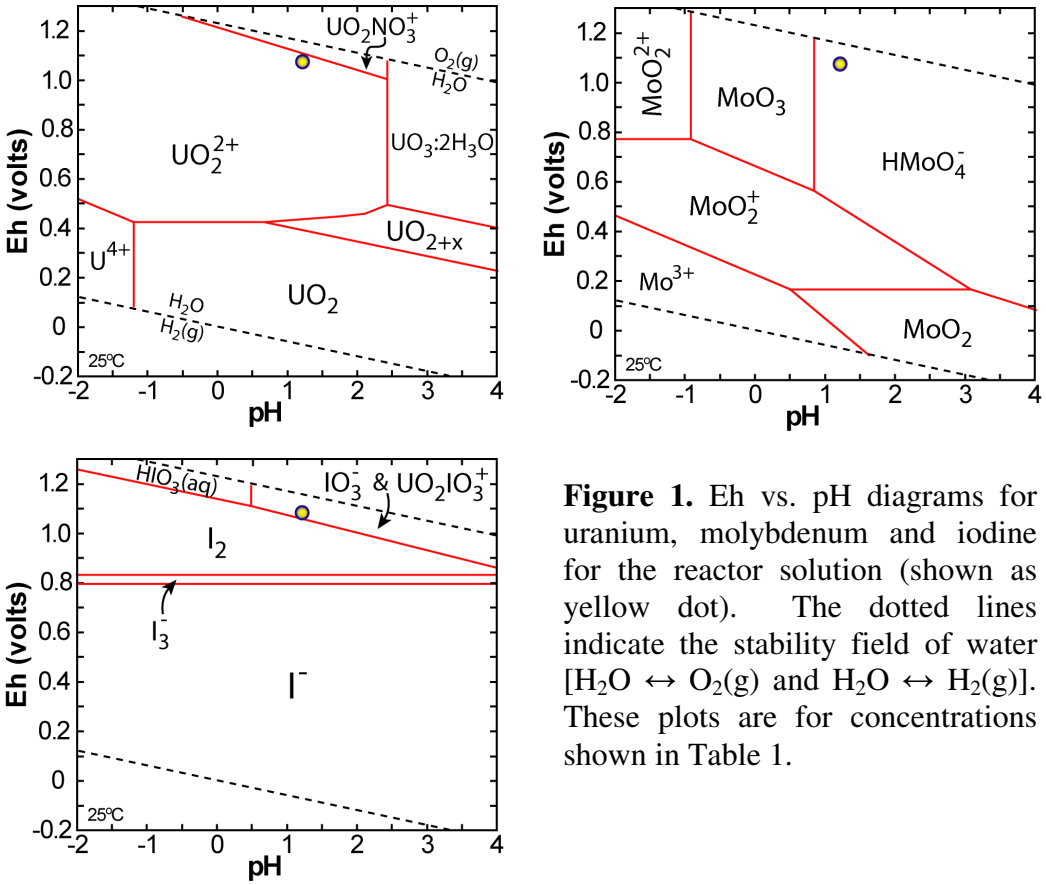

Figure 1. Eh vs. pH diagrams for uranium, molybdenum and iodine for the reactor solution (shown as yellow dot). The dotted lines indicate the stability field of water [$H_2O \leftrightarrow O_2(g)$ and $H_2O \leftrightarrow H_2(g)$]. These plots are for concentrations shown in Table 1.

The Geochemist's Workbench code was used to simulate the change in speciation and saturation state of the reactor solution with increasing pH. Processes that could drive the solution pH to higher values during reactor operation include: the radiolytic destruction of nitrate and subsequent loss of nitrogen as a gaseous species as well as the corrosion of steel walls of the reactor vessel and components. For both processes the pH increases steadily as either nitrogen is "titrated" out of the system or iron is titrated into the system. These processes can be summarized by the following general reactions:

$$NO_3^- + H^+ \rightarrow 0.5H_2O + 0.5N_2(g) + 1.25O_2(aq) \quad (1)$$

$$Fe + 3H^+ + 0.75O_2(aq) + NO_3^- \rightarrow FeNO_3^{2+} + 1.5H_2O \quad (2)$$

The increase in pH is countered by hydrolyses of the uranyl and ferric ions (reactions 3 and 4) as well as by the precipitation of ferric hydroxides or oxides (reactions 5 and 6), uranyl oxide hydrate (reaction 7) and possibly uranyl peroxide (reaction 8); if the steady state concentration of radiolytic hydrogen peroxide is high enough ("s" indicates solid).

$$2UO_2^{2+} + 2H_2O \leftrightarrow (UO_2)_2(OH)_2^{2+} + 2H^+ \quad (3)$$

$$2H_2O + 2FeNO_3^{2+} \leftrightarrow Fe_2(OH)_2^{4+} + 2NO_3^- + 2H^+ \quad (4)$$

$$FeNO_3^{2+} + 3H_2O \leftrightarrow Fe(OH)_3(s) + 3H^+ + NO_3^- \quad (5)$$

$$2FeNO_3^{2+} + 3H_2O \leftrightarrow Fe_2O_3(s) + 6H^+ + 2NO_3^- \quad (6)$$

$$UO_2^{2+} + 3H_2O \leftrightarrow UO_3{:}2H_2O(s) + 2H^+ \quad (7)$$

$$UO_2^{2+} + 4H_2O + H_2O_2 \leftrightarrow UO_2O_2{:}4H_2O(s) + 2H^+ \quad (8)$$

Results from simulations of the pH increase that could be caused by reactions 1 and 2 are shown in Figure 1. The dotted lines in these plots show how the pH increase would be counteracted (buffered) by the precipitation of uranyl oxide hydrate and ferric hydroxide (reactions 5 and 7). These models predict that the pH of the reactor solution could increase to values as high as 3.0 depending on precipitation kinetics. Other speciation models were run for the reactor solution (Table 1) for a pH range extending from -2 (slightly lower than concentrated nitric acid) to 4 (a conservative high end of possible pH envelop for the reactor solution).

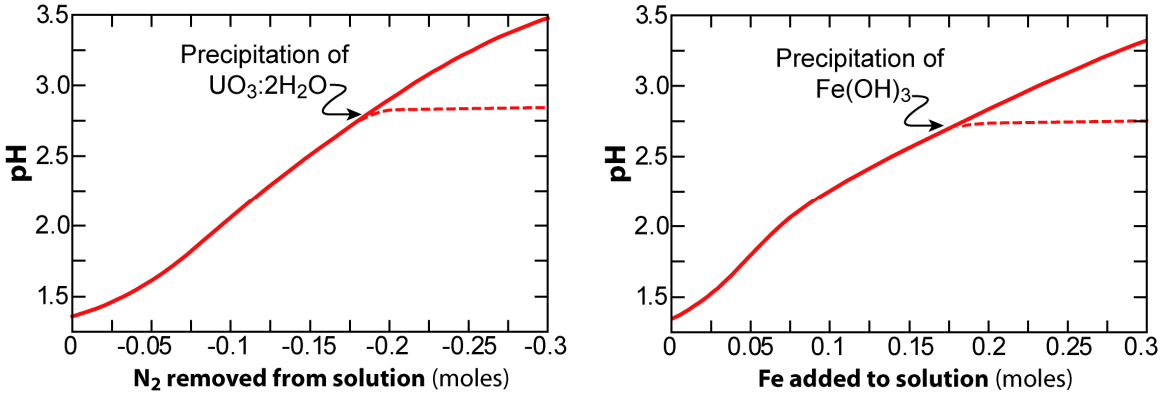

Figure 2. Increase in pH of reactor solution due to nitrogen loss to off-gas (left, solid line, reaction 1) and iron dissolution to form ferric nitrate (right, solid line, reaction 2). The pH increase is counteracted by precipitation reactions (dotted lines, reactions 5 and 7).

Results showing the saturation state and speciation of molybdenum over the pH range -2 to 4 are shown in Figure 3. These plots highlight how the uncertainty in thermodynamic data can significantly affect the predicted speciation of the solution. For example Figure 3a shows the saturation indices for the two key uranium solids. The model predicts that the reactor solution would become saturated with respect to uranyl oxide hydrate at a pH around 3; however, there is uncertainty as to the solubility product (K_{sp}) of uranyl molybdate. Sparse experimental data (e.g.

[5], [6]) suggest the $\log_{10}K_{sp}$ for uranyl molybdate falls in the range of -13 to -15 (for the basis reaction: $UO_2MoO_4(s) \leftrightarrow UO_2^{2+} + MoO_4^{2-}$). When the model is run using $\log_{10}K_{sp}$ = -15 the reactor solution becomes saturated with uranyl molybdate at pH 1; however if $\log_{10}K_{sp}$ = -13, then uranyl molybdate is not predicted to precipitate in this system (Figure 3a) (remains slightly undersaturated).

Figure 3b shows the saturation indices for the two key molybdenum solids. The model predicts that the reactor solution would become saturated with respect to molybdenum oxide at a pH around pH -0.5; however there is uncertainty as to the K_{sp} for zirconium molybdate. Some experimental data suggest that the $\log_{10}K_{sp}$ for uranyl molybdate fall in the range of -34 to -36 (for the basis reaction: $Zr(MoO_4)_2(s) \leftrightarrow Zr^{4+} + 2MoO_4^{2-}$). When the model is run using $\log_{10}K_{sp}$ = -36 the reactor solution becomes saturated with zirconium molybdate at pH = 0.5; however if $\log_{10}K_{sp}$ = -34, then zirconium molybdate is not predicted to precipitate in this system (Figure 3b). Figure 3c shows molybdenum speciation for a case in which molybdenum oxide and uranyl molybdate precipitate. Molybdenyl(VI) is predicted to be the main species at low pH and its concentration drops from $1x10^{-5}$ molar down to $1x10^{-6.5}$ molar due to the precipitation of molybdenum(VI) oxide. Above pH = 0, hydrogen molybdate becomes the dominant molybdenum species; however zirconium molybdate is also predicted to be a significant species around pH 1 (concentration of zirconium molybdate is dotted to signify uncertainty in its stability constant). With the precipitation of uranyl molybdate, the hydrogen molybdate concentration decreases from a maximum of $1x10^{-6.75}$ molar at pH = 0.5, to a minimum of around $1x10^{-7}$ molar around pH = 3. Figure 3d shows molybdenum speciation for a case in which molybdenum oxide and zirconium molybdate precipitate, but uranyl molybdate does not. Again, molybdenyl(VI) is predicted to be the main species at low pH and its concentration drops from $1x10^{-5}$ molar down to $1x10^{-6.5}$ molar due to the precipitation of molybdenum(VI) oxide. Above pH = 0, hydrogen molybdate becomes the dominant molybdenum species; however zirconium molybdate is also predicted to be a significant species around pH 1. Around pH 1.5 the concentration of hydrogen molybdate drops to a value of approximately $1x10^{-6}$ molal due to the precipitation of zirconium molybdate.

Figure 3e shows molybdenum speciation for a case in which none of the solids precipitate (perhaps due to kinetic inhibitions). This plot reiterates the dominance of molybdenyl(VI) at low pH and hydrogen molybdate above a pH value of zero. Figure 3f shows that uranium speciation is dominated by uranyl nitrate and the uranyl ion at low pH, and by uranyl hydroxides at higher pH.

Another potentially important precipitate is the uranyl peroxide solid studtite (UO_2O_2:$4H_2O$). Key thermodynamic properties of this mineral have been quantified [7]; however, its importance in the reactor solution is unknown due to uncertainties in the steady-state concentration of hydrogen peroxide in the irradiated fuel during reactor operation. It is anticipated that hydrogen peroxide will be produced during reactor operation by radiolysis of water. Depending on the ratio of the rates of hydrogen peroxide formation and auto destruction, a steady state concentration will be established. If this concentration is high enough, it could cause uranium to precipitate as the sparingly soluble uranyl peroxide studtite at a pH value less 3.0. The model results in Figure 4 establish the pH range over which uranyl peroxide precipitation may occur for a given steady state concentration of hydrogen peroxide.

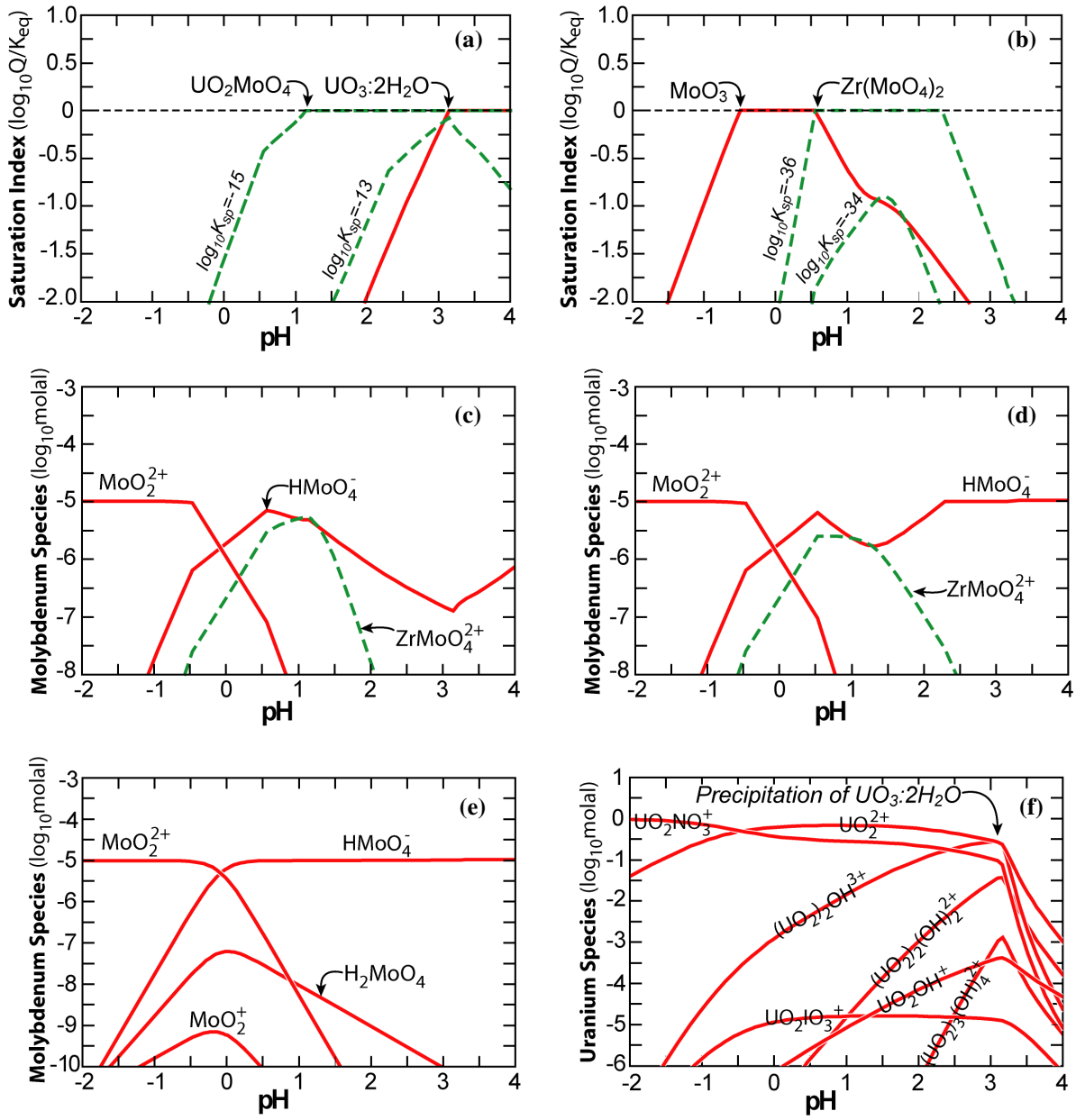

Figure 3. Speciation of reactor solution as a function of pH (compositions from Table 1, Eh from Table 2). (a) Mineral saturation index plot for key uranium solids (see text above for discussion). (b) Mineral saturation index plot for key molybdenum solids. (c) Molybdenum speciation for the case where molybdenum oxide and uranyl molybdate precipitate. (d) Molybdenum speciation for the case where molybdenum oxide and zirconium molybdate precipitate. (e) Molybdenum speciation diagram for the case where no minerals precipitate. (f) Uranium speciation plot showing increased concentrations of uranyl hydroxide species with increasing pH, and the precipitation of uranyl oxide hydrate around pH = 3.

The plot on the left of Figure 4 shows the stability of uranyl peroxide in terms of hydrogen peroxide molality and pH. It predicts that, at a hydrogen peroxide concentration as low as approximately $1x10^{-7}$ molar, uranyl peroxide may be stable at a pH around 2.5. At higher hydrogen peroxide concentrations the pH stability threshold decreases. For example, as shown in the plot on the right of Figure 4, the reactor solution could become saturated with respect to uranyl peroxide at a pH as low as 0.5 if the steady state concentration of hydrogen peroxide is $1x10^{-3}$ molar or as high as pH = 2 if the concentration is $1x10^{-6}$ molar. More information about the rate of hydrogen peroxide production and auto destruction is needed to accurately predict the significance of uranyl peroxide precipitate during uranyl solution reactor operation.

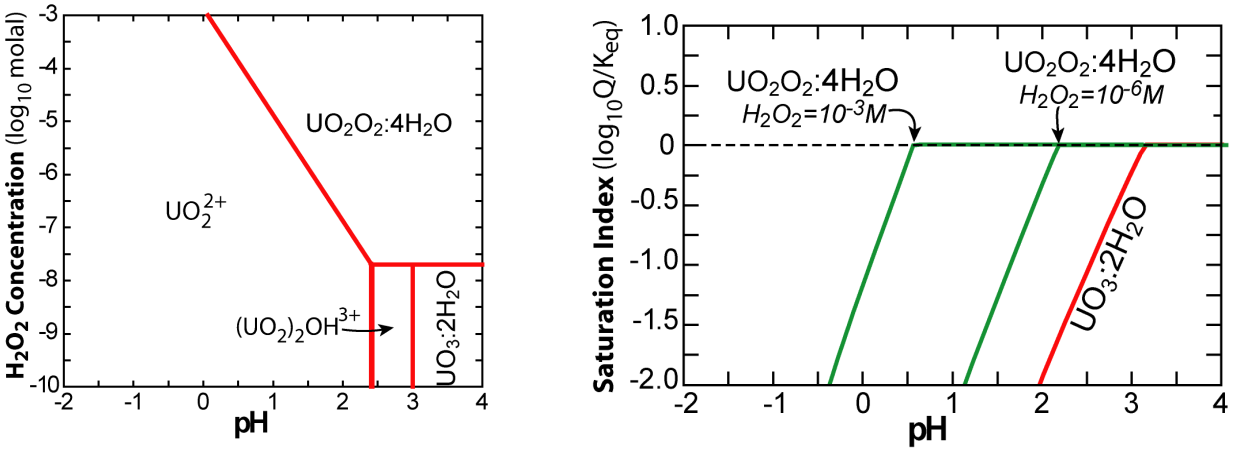

Figure 4. Left: stability of the uranyl peroxide mineral studtite in terms of the concentration of hydrogen peroxide and pH. Right: saturation index for uranyl peroxide and uranyl oxide hydrate vs. pH for 10^{-3} and 10^{-6} molar H_2O_2 for the reactor solution shown in Table 1.

4. Conclusions

The thermodynamic modeling presented in this paper has identified four processes that could adversely affect ^{99}Mo production from a uranyl nitrate solution reactor: (1) Fission product anions such as TcO_4^-, IO_3^-, I^-, Br^-, $HSeO_4^-$ and SeO_4^{2-}, that accumulate during burn-up (Table 2), may compete with $HMoO_4^-$ or MoO_4^{2-} on anion exchange resins and might lower the molybdenum separation efficiency and influence product purity. If experiments show this phenomenon to be a significant issue, it can be counteracted by reprocessing the fuel solution at regular intervals to remove competing species. (2) The loss of nitrate from the solution due to radiolysis and the corrosion of iron bearing vessel components are expected to cause the pH of the reactor solution to increase to a value at which the solution is saturated with respect to uranium and molybdenum solids. Such an increase in pH could be counteracted by adding nitric acid to the solution to compensate for nitrogen loss and by using metals that are resistant to corrosion (e.g., zirconium-based alloys) for vessel component construction. (3) The reactor solution could become saturated with respect to uranyl molybdate and/or zirconium molybdate at pH values as low as 1. However, experimental studies are needed before the significance of uranyl or zirconium molybdate precipitation can be fully quantified. (4) If the steady state concentration of hydrogen peroxide in the reactor reaches values near $1x10^{-3}$ molar the uranyl peroxide solid studtite (UO_2O_2:$4H_2O$) could precipitate at pH values less than 1. However, if the steady state concentration of hydrogen peroxide is $1x10^{-6}$ molar or lower, then the solution is

predicted to become saturated with respect of uranyl peroxide at a pH value around 2. If experiments indicate that uranyl peroxide precipitation is an issue for reactor operation, the process could be counteracted by adding a material that catalyzes the auto destruction of hydrogen peroxide.

Areas for future research identified in this study are: performing experiments (especially studies accounting for kinetics and thermal effects) to confirm the theoretical results highlighted above. Specifically work needs to focus on quantifying the solubility constants for uranyl and zirconium molybdates, quantifying the stability constants of zirconium molybdate species and quantifying the steady state concentration of hydrogen peroxide during reactor operation. Overall these modeling results should only be looked at as guides to prioritizing experimental work.

5. Acknowledgements

The submitted manuscript has been created by UChicago Argonne, LLC, Operator of Argonne National Laboratory ("Argonne"). Argonne, a U.S. Department of Energy Office of Science laboratory, is operated under Contract No. DE-AC02-06CH11357. The U.S. Government retains for itself, and others acting on its behalf, a paid-up nonexclusive, irrevocable worldwide license in said article to reproduce, prepare derivative works, distribute copies to the public, and perform publicly and display publicly, by or on behalf of the Government. Work supported by the U.S. Department of Energy, National Nuclear Security Administration's (NNSA's) Office of Defense Nuclear Nonproliferation, under Contract DE-AC02-06CH11357.

6. References

[1] Personal communication with Gary Neeley of Babcock & Wilcox Technical Services Group, January, 2008

[2] T. J. Wolery and S. A. Daveler, "EQ6, A Computer Program for Reaction Path Modeling of Aqueous Geochemical Systems: Theoretical Manual, User's Guide, And Related Documentation (Version 7.0)," Lawrence Livermore National Laboratory Report UCRL-MA- 110662 PT IV, 1992.

[3] Bard, Parsons, Jordan, 1985, Standard Potentials in Aqueous Solution (Dekker, New York, 1985)

[4] Martell, A. E., Smith R. M., Motekaitis, R. J., 2004, NIST Standard Reference Database 46, Version 8.0

[5] S. Prasad and J. V. Barros, "Electrometric studies on uranyl molybdates as a function of pH," Eclética Química, Volume 23, Pages 1-12, 1998

[6] L. M. Ferris, "Solubility of Molybdic Oxide and its Hydrates in Nitric Acid, Nitric Acid-Ferric Nitrate, and Nitric Acid-Uranyl Nitrate Solutions, Journal Of Chemical And Engineering Data, Volume 6, Pages 600-603, 1961

[7] K. H. Kubatko, K. B. Helean, A. Navrotsky, P. C. Burns, "Stability of Peroxide-Containing Uranyl Minerals," Science Volume 302, Pages 1190-1193, 2003